IEEE Access
Multidisciplinary | Rapid Review | Open Access Journal

Received July 14, 2019, accepted July 27, 2019, date of publication August 5, 2019, date of current version August 28, 2019.

Digital Object Identifier 10.1109/ACCESS.2019.2933025

Impact of Atmospheric Parameters on the Propagated Signal Power of Millimeter-Wave Bands Based on Real Measurement Data

CONGZHENG HAN[1,2,3], (Senior Member, IEEE), AND SHU DUAN[1,4]

[1]Key Laboratory of Middle Atmosphere and Global Environment Observation, Institute of Atmospheric Physics, Chinese Academy of Sciences, Beijing 100029, China
[2]College of Earth and Planetary Sciences, University of Chinese Academy of Sciences, Beijing 100049, China
[3]School of Electronic Engineering, Chengdu University of Information Engineering, Chengdu 610225, China
[4]Jiangsu Key Laboratory of Meteorological Observation and Radar Technology, Nanjing 211006, China

Corresponding author: Congzheng Han (c.han@mail.iap.ac.cn)

This work was supported in part by the National Natural Science Foundation of China under Grant 41605122, and in part by the Chinese Academy of Sciences under Grant 2018VTA0013.

ABSTRACT Millimeter waves have been recognized as carriers for 5G cellular networks. We carried out a series of millimeter-wave measurements in Beijing, China, and studied the atmospheric impacts on millimeter-wave transmission. Our measurement design is an exemplary LOS transmission link. We also studied a 3 km long commercial E-band millimeter-wave backhaul link in Göteborg, Sweden. We monitored the variation of received signal in the rain, and compared the theoretical rain-induced signal attenuation with the practically monitored signal attenuation. Our results show that there is 1.5–4.5 dB uncertainty between the practical and theoretical rain-induced signal attenuation. Assuming the prediction of rain intensity is available, we have proposed a novel rain-aware radio resource management strategy which adapts the modulation and coding schemes of an OFDM system to rainfall events. We have applied the proposed algorithm to an OFDM - based 5G system, and the throughput result is improved. The result shows that the throughput of a fixed modulation and coding scheme system is between 12%–95% of the system employing the proposed algorithm during rainfall events.

INDEX TERMS Atmospheric attenuation, millimeter-wave radio propagation meteorological impact, radio resource management, adaptive modulation and coding, 5G.

I. INTRODUCTION

Provided the significant increase in bandwidth and new capabilities offered by millimeter wave frequencies, the base station-to-device links, as well as backhaul links between base stations, will be able to handle much greater capacity than today's cellular networks in populated areas [1]–[3].

Governments around the world have allowed operations in the millimeter bands for backhaul, often as little or no licensing fee. Backhaul communications are typically used throughout the 2 to 6 GHz frequency bands, but they are becoming increasingly popular at various licensed and unlicensed bands in the 18, 22, 28, 33, 38 - 40, 42, 50, and 60 GHz bands throughout the world. Recently, the E-bands at 71-76, 81-86, and 92-95 GHz in the USA have become popular, as the spectrum is made available at very little cost to carriers [4]–[6]. Millimeter-wave wireless backhauls can be rapidly deployed compared to fiber backhauls and less expensive. The latest report from Ericsson [7] has indicated that 40 percent of backhaul connections globally (including China) are expected to be based on microwave technology by 2023. Even higher millimeter frequencies may be of interests to support the evolution of mobile broadband backhaul beyond 2020, such as the frequency range 92-114.5 GHz (W-band) and 141-174.8 GHz (D-band) [8].

A major challenge for the millimeter-wave technology is its sensitivity to the propagation environment [9]–[11]. One of the limiting factors is that the attenuation due to rain affects the reliable communication system operating at frequency above 10 GHz. The current cellular networks operate between 800 MHz to 2.6 GHz. The electromagnetic signals are less affected by atmospheric conditions for lower frequencies, as shown in Fig. 2 in the later section. It is

The associate editor coordinating the review of this manuscript and approving it for publication was Cunhua Pan.

expected that the future cellular systems may use millimeter-wave frequencies as an addition to the currently saturated lower spectrum bands for wireless communications [12]. The latest WRC-19 document [5] states that 24-86 GHz bands will be considered for 5G. Many countries have already started to deploy commercial 5G networks with a particular focus on the spectrum range 26.5 GHz to 29.5 GHz while waiting for 5G regulations and specifications to be completed. Although millimeter-wave radio propagation measurements have been carried out all over the world, but rarely measurements and papers concern the additional modeling components such as atmospheric parameters. As millimeter-waves have been traditionally used for radar and military applications, the scenarios for commercial cellular networks in changing weather conditions have not been studied much. However, it is becoming an important topic. The current release 14 of 3GPP TR 38.901 document has addressed the impacts of oxygen absorption for frequencies between 53 and 67 GHz as an additional modeling component to the channel model (section 7.6). In the ETSI white paper [13], it introduced a series of millimeter-wave measurements in different parts of the world in rainy weather. During Globecom conference in 2018, the workshop ''Channel Models and Measurements for MMwave bands'' particularly emphasized that ''Even though the latest channel model has already been extended to 100 GHz by 3GPP, rarely papers concern the new modelling components such as oxygen absorption, large bandwidth, large antenna array, spatial consistency.''

It has been long known that microwave attenuation by rainfall near wavelength of 1 cm is nearly linearly related to rainfall rate based on the work by Atlas [14]. It is shown that at frequencies of about 35 GHz, a power-law relationship between the rain intensity and signal attenuation is approximately linear and is essentially independent of drop size distribution (DSD) and temperature, showing empirical errors of less than 10%. Zhao *et al*. [15] conducted millimeter-wave frequency links with a length of 230 m at 35 GHz and 390 m at 103 GHz to examine rain specific attenuation with simultaneous measurement of rain rate distribution. It shows among different rain DSDs, Weibull distribution has a good agreement with the local experiment. 25 GHz and 38 GHz frequencies have been used for building communication links to monitor rain induced attenuation [16], [17]. In the trial in Australia [17], the actual signal attenuation was found to be a lot higher than the expected rain induced attenuation. Contribution from wind, wet antenna, and the availability of reliable long-term local data for building local rain attenuation mathematical model need to be considered to improve the accuracy of rain estimation using microwave links. In [6], the authors included the rain attenuation parameter based on ITU rain model to large-scale MIMO channel model for millimeter-wave transmission at E band (71-76 GHz and 81-86 GHz) for small-cell backhaul in dense urban environment. Our paper considers a similar channel scenario, and we will show signal attenuation in real time measurement compared to ITU rain model.

There have been few recorded measurements for studying the characteristics of wireless backhauls and transmission links in rainy weather in China. The authors of this paper presented the measurements from a short millimeter-wave transmission link of 80 m at 25 GHz during rainy weather in summer of 2016 in Beijing [18]. Compared to the previous work, the experiment presented in this paper was conducted over a longer distance of 700 m for a selection of 5G frequencies including 23/25/28/38 GHz. An experiment of commercial E-band (72.625 GHz and 82.625 GHz) backhaul link in Göteborg, Sweden during summer in 2017 was also presented in this paper. This paper provides a comprehensive study on the atmospheric effects on near ground millimeter-wave transmission and backhaul links, and on the throughput performance of millimeter-wave wireless systems. We have also proposed a rain-aware radio resource management strategy to improve the system performance. The contributions and organization of this paper can be summarized as follows:

1) We present a series of millimeter-wave tests designed to be an example of LOS base station to user device link at the institute of Atmospheric Physics, Beijing, China during summer of 2017 and April 2018. The test can also represent a millimeter-wave backhaul link. The link frequencies are at 23 GHz, 25 GHz, 28 GHz, and 38 GHz. We also analyse the impact of rain on a commercial E-Band millimeter-wave backhaul link at 72.625 GHz and 82.625 GHz in Göteborg, Sweden during 7-17 June 2017.

2) We study the empirical atmospheric attenuation model for calculating the signal attenuation due to water vapour, oxygen, rain, and other-than-rain precipitation. Based on the recordings from the weather station and disdrometer, we work out the signal attenuation theoretically and compare with the practically monitored signal attenuation. The gap between the theoretical and practical measurement is analyzed.

3) Based on a 5G simulator, we investigate the block error rate and throughput performance of different combinations of modulation and coding schemes. We propose a dynamic rain-aware link adaptation algorithm to overcome the atmospheric attenuation. We then analyze the performance of the proposed algorithm. Based on the assumption that the rain intensity can be predicted, appropriate parameters can be selected to achieve high data rate.

4) We propose that rain can be added as an additional modeling component to the current millimeter-wave channel model in addition to oxygen absorption. The results also show that the cellular network performance can be improved if local meteorological agencies can collaborate with the local network operators and provide real time weather information and prediction.

This paper is organized as follows. In section II, we present an overview of the characteristics of millimeter-wave propagation and the impacts of various atmospheric factors on the millimeter-wave signal strength. Section III details measurement setup and methods of performance evaluation. In section IV, we present the proposed rain-aware radio resource management algorithm for 5G system and

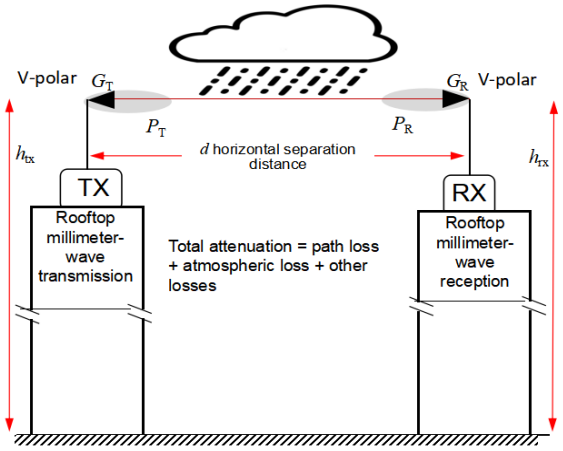

FIGURE 1. Illustration of the millimeter-wave signal transmission.

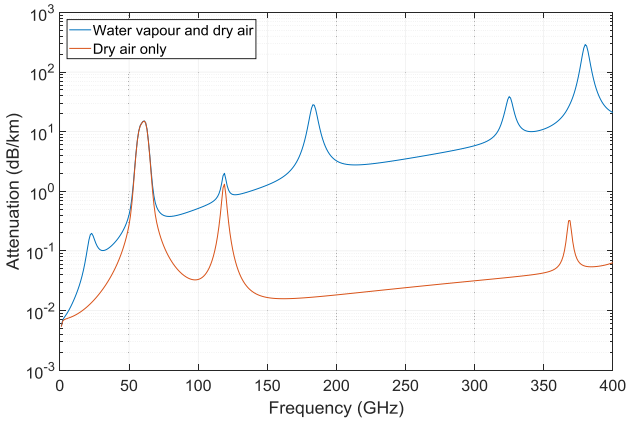

FIGURE 2. Frequency dependent attenuation of electromagnetic radiation in standard atmosphere (barometric pressure 1013 mbar, temperature 15 °C, and water vapour density of 7.5 g/m3).

demonstrate its performance using the recordings from several rainfall events. Finally, the conclusions are given in section V.

II. MILLIMETER-WAVE PROPAGATION AND PREDICTION OF ATMOSPHERIC ATTENUATION

A. MILLIMETER-WAVE PROPAGATION

The millimeter-wave signal transmission is illustrated in Fig. 1. For a point-to-point LOS millimeter-wave link, by considering equations (1), (2), and (5), the received power P_R can be written as:

$$P_R = P_T + G_T + G_R - PL - AL - OL \tag{1}$$

where P_T (dB) and P_R (dB) are transmit and receive signal power, G_T (dBi) and G_R (dBi) are transmitter and receiver antenna gain, PL (dB) is the propagation path loss (2), AL (dB) is the atmospheric loss (5), and OL(dB) refers to other losses. The propagation path loss can be expressed as [1]:

$$PL(f_c, d) = 32.4 + 20log10(f_c) + 10nlog10(d/d_0) + \chi_\sigma, \quad d \geq 1m \tag{2}$$

where f_c denotes the carrier frequency in GHz, d is the transmitter and receiver separation distance, the reference distance d_0 is 1m, n represents the path loss exponent. χ_σ is a zero-mean Gaussian random variable with a standard deviation σ in dB.

B. ATMOSPHERIC ATTENUATION

Atmospheric attenuation is important for millimeter-wave propagation, and the absorptive attenuation of radio waves by atmospheric molecules is mainly due to the presence of oxygen and water vapour. The atmospheric loss is generally defined in terms of decibels (dB) loss per kilometer of propagation. Since the fraction of the signal loss is a strong function of the distance travelled, the actual signal loss experienced by a specific millimeter-wave link due to atmospheric effects depends directly on the length of the link. A simplified model describing the attenuation of millimeter-wave for the range of 1 GHz to 100 GHz through atmosphere AL can be described as follows:

$$AL = A_r + A_v + A_o + A_p(dB) \tag{3}$$

which includes primarily the attenuation effects of dry air (including oxygen), humidity, fog and rain. A_r refers to the attenuation caused by rain, A_v represents the water vapour attenuation, A_o represents the attenuation due to dry air, and A_p is the attenuation as a result of other-than-rain precipitation (i.e. fog, sleet, snow).

Other causes of losses (OL) include: the coaxial cable loss at transmitter and receiver; the stability of the transmit and receive signal terminals (equipment, circuits etc) may be affected by temperature and water vapor variations, causing additional attenuation; a thin film of water on the transmit and receive antenna can cause considerable attenuation, referred here as ''wet antenna attenuation''; anything that obstructs the LOS channel may introduce additional loss.

1) DRY AIR AND WATER VAPOUR ATTENUATION

Attenuation due to absorption by oxygen and water vapour is always present and should be included in the calculation of total propagation loss at frequencies above about 10 GHz. For millimeter frequency range, the resonance lines for water vapour and oxygen are at 22.3 / 183.3 / 323.8 GHz and 60 GHz / 118.74 GHz.

To illustrate the electromagnetic signal attenuation due to meteorological factors such as dry air and water vapour, Fig. 2 was plotted based on the equations given in [15], [19] for a given barometric pressure and temperature. The first excess attenuation occurs at around 22 GHz due to water vapour, and the second at 60 GHz due to oxygen. Oxygen absorption has a maximum attenuation at 60 GHz, and contributes to 7-15 dB / km in the received signal strength at the frequency range of 57-63 GHz.

The specific attenuation due to water vapour and dry air can be estimated using Recommendation ITU-R P.676-10,

TABLE 1. Signal loss due to different atmospheric parameters.

Atmospheric Parameter			Signal Loss (dB) per km				
			28GHz	38 GHz	60 GHz	73 GHz	83 GHz
Humidity	**Classification**	**Humidity level**					
	Dry	20%	0.028	0.025	0.050	0.074	0.095
	Average	45%	0.068	0.062	0.129	0.184	0.236
	Humid	90%	0.148	0.143	0.305	0.446	0.547
Rain	**Classification**	**Rain rate**					
	Very light rain	R<1 mm/h	< 0.2	< 0.4	< 0.9	< 1.1	<1.2
	Light rain	1 mm/h≤R<2 mm/h	< 0.4	< 0.7	< 1.4	< 1.8	<2.0
	Moderate rain	2 mm/h≤R<5 mm/h	< 0.9	< 1.5	< 2.8	< 3.4	<3.7
	Heavy rain	5 mm/h≤R<10 mm/h	< 1.7	< 2.75	< 4.77	< 5.6	<6.0
	Very heavy rain	10 mm/h≤R<20 mm/h	< 3.2	< 5.0	< 8.0	< 9.1	<9.7
	Extreme rain	R ≥20 mm/h (e.g. 50 mm/h)	≥ 3.2 (7.4)	≥ 5.0 (10.9)	≥ 8.0 (15.9)	≥ 9.1 (17.6)	≥9.7 (18.4)
Fog (15° C)	**Classification**	**LWD value**					
	Dense Fog	Visibility <1km, LWD≥0.1mg/m^3	0.046-0.230	0.083-0.413	0.191-0.956	0.268-1.340	0.331-1.653
	Light Fog	LWD≤0.0.05mg/m^3	⩽0.230	⩽0.413	⩽0.096	⩽0.134	⩽0.165
	Mist	Visibility (1km-10km), LWD≥0.01mg/m^3	0.005-0.230	0.008-0.413	0.019-0.956	0.027-1.340	0.033-1.626
	Wet haze	Visibility<1km, LWD<0.1mg/m^3	<0.046	<0.083	<0.191	<0.268	<0.331
	Haze	Visibility (1km-10km), LWD<0.01mg/m^3	<0.005	<0.008	<0.019	<0.027	<0.033

2013 [20]:

$$\gamma = A_v + A_o(\text{dB/km}) \tag{4}$$

A_v: The specific attenuation due to water vapour (dB/km)
A_o: The specific attenuation due to dry air (dB/km)

$$\gamma = 0.1829 f N^{"}(\text{dB/km}) \tag{5}$$

where $N^{"} = N^{"}(p, T, \rho, f)$ is the imaginary part of the complex refractivity, and it is a function of the pressure p (hPa), temperatures T(°C) and the water vapour density ρ (g/m^3).

$$N^{"} = \sum_i S_i F_i + N_D^{"} \tag{6}$$

The Si is the strength of the i-th line, F_i is the line shape factor. $N_D^{"}(f)$ is the dry continuum due to pressure-induced nitrogen absorption and the Debye spectrum.

Fig. 3 shows the signal attenuation per 1 km for the frequency range between 0 and 100 GHz due to water vapour at different humidity levels. A higher humidity percentage indicates air-water mixture is more humid. The signal attenuation as a result of water vapour for various frequencies is detailed in Table 1. For a comfortable, and healthy space, humidity levels should be between 30 to 50 %, with the ideal level being about 45 %. The excessive attenuation peak due to water vapour is at around 22.235 GHz, causing up to 0.3 dB/km signal attenuation. For other frequencies below 38 GHz, the signal attenuation due to dry air and water vapour is less than 0.2 dB for a 1 km link length. For signals at E-band (71 - 86 GHz), the attenuation due to humidity is larger than 0.45 dB/km.

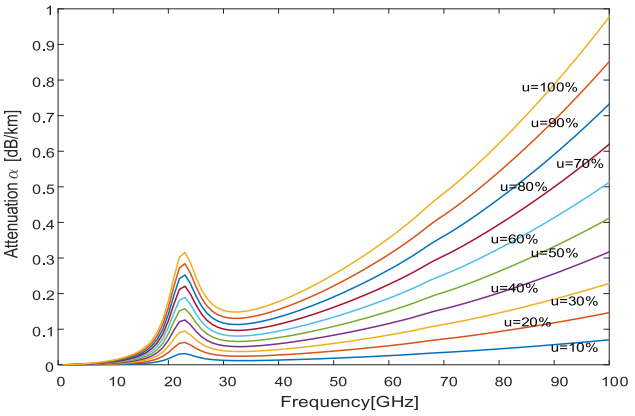

FIGURE 3. The attenuation caused by water vapour (H2O) (barometric pressure 1013 mbar and temperature 15 °C).

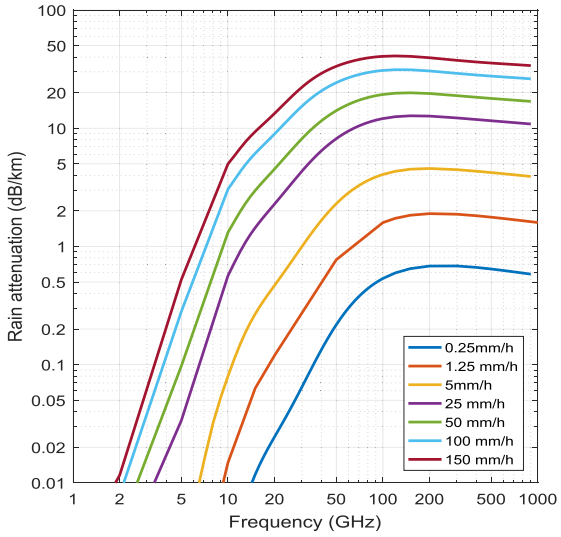

FIGURE 4. Rain attenuation in dB/km across frequency at various rainfall rates.

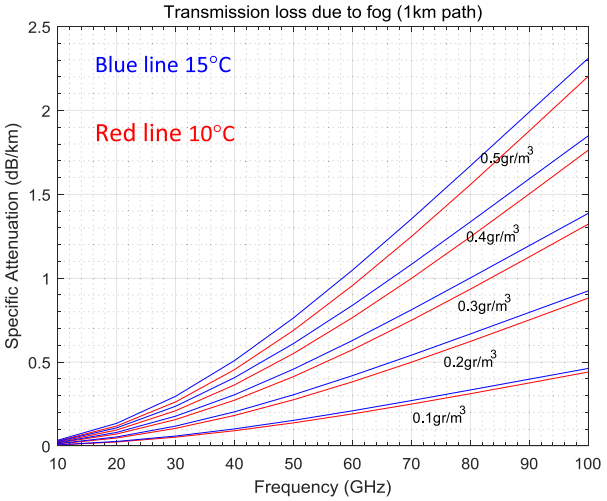

FIGURE 5. The attenuation due to fog at typical LWCs (barometric pressure 1013 mbar and temperature 10 / 15 °C).

2) RAINFALL EFFECTS ON RADIO SIGNALS

A power law empirical model is often used in the calculation of rain induced attenuation A_r and the rain rate R [21]:

$$A_r = aR^b(d/1000)(\text{dB}) \tag{7}$$

where the constants a and b are related to frequency, rain temperature, the rain drop size distribution, and polarization depending on rain attenuation model. In our study, d (m) is the length of the microwave link, and A_r is the overall signal attenuation induced by rain between the transmitter and receiver. A set of commonly used power-law coefficients can be found in ITU-R P. 838-3 [22].

Assuming vertical polarization, the rain attenuation across millimeter frequency band at various rainfall rates is shown in Fig. 4. The numerical values of rain induced signal attenuation are given in Table 1. Compared to other atmospheric factors, atmospheric attenuation due to rain is one of the most noticeable components of excess losses, it is not important for low frequency bands, but as the frequency increases, it can become of increasing concern especially at frequencies of 10 GHz and above [23]. For a heavy rainfall event, a 38 GHz signal links will experience around 7.5 dB loss per km, and as the frequency increases to 73 GHz, the signal loss becomes 12 dB per km.

3) OTHER-THAN-RAIN PRECIPITATION

Other than rain precipitation, attenuation can also occur as a result of absorption and scattering by such as snow, sleet, hail and fog.

The specific attenuation due to fog (or cloud) is given in ITU-R P.840-6 [24]:

$$\gamma_c = K_l M(\text{dB/km}) \tag{8}$$

where:

γ_c: specific attenuation (dB/km) within the fog (or cloud)

K_l: specific attenuation coefficient ((dB/km)/(g/m^3))

M: liquid water density (LWD) in the fog (or cloud) (g/m^3).

At frequencies of the order of 100 GHz and above, attenuation due to fog may be significant. The liquid water density in fog is typically about 0.05 g/m^3 for medium fog (visibility of the order of 300 m) and 0.5 g/m^3 for thick fog (visibility of the order of 50 m). Fig. 5 describes the signal attenuation per 1 km at frequencies of up to 100 GHz due to fog at typical liquid water density levels. The fog-induced attenuation increases with increasing frequency, and can be classified using the level of liquid water contents and visibility levels as shown in Table [25]. The typical liquid water contents ranging between 0.01 and 0.4 g/m^3 [26]. Higher level of LWD decreases visibility and indicates dense fog.

In the microwave and millimeter-wave bands, attenuation due to dry snow is usually negligible. For wet snow, millimeter-waves can be attenuated significantly in the melting layer in high latitude regions [28]. Recommendation ITU-R P.530-13 provides a prediction model for the fading due to wet snow on low-elevation, terrestrial microwave links [27].

The amplification factor Γ (Δh) for calculating the combined rain and wet snow attenuation (referred here as 'sleet') is a function of link height (altitude of the middle of the radio link in meters) and the rain height (360 m above the zero-degree isotherm). The amplification factor is the specific attenuation experienced from combined rain and wet snow divided by the specific attenuation of the equivalent rain. Fig. 6 indicates that the amplification factor equals to 1 below the melting layer, the sleet have the similar specific attenuation as rain [29], and the sleet affects the microwave radiation similar to the effects caused by rain [30]. The sleet DSD may be different from the DSD of rain particles [31]. As an example, for our measurement location, the altitude of the millimeter-wave link is 51 m, and the zero-degree isotherm is around 4675 m, and therefore any sleet effect can be treated using rain attenuation model.

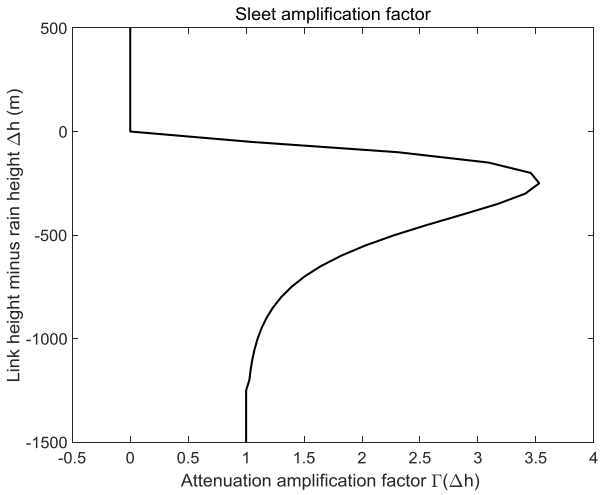

FIGURE 6. Variation of sleet amplification factor $\Gamma(\Delta h)$ as a function of altitude relative to the rain height.

C. ATMOSPHERIC LOSS AS ADDITIONAL MODELLING COMPONENTS

The millimeter-wave channel model is expected to take care of propagation aspects such as blocking and atmosphere attenuation. For millimeter-wave channel modeling, the current release 14 of 3GPP TR 38.901 [32] considers the impacts of oxygen absorption for frequencies between 53 and 67 GHz as an additional modeling component to the channel model. For the frequency range of 0 to 100 GHz, the maximum attenuation due to oxygen absorption occurs at 60 GHz with 15 dB loss.

The water vapour attenuation A_v is insignificant compared to oxygen absorption, and the maximum attenuation is less than 1 dB / km for up to 100 GHz. However, the impact of rain, hail, sleet or snow can also cause large attenuation for high frequency bands. For heavy rains, the rain-induced attenuation is comparable to the oxygen absorption attenuation in the millimeter-frequency range as already been discussed in II.B (2). We suggest that the frequency dependent rain attenuation $A_r(f_c)$(dB/km) can be calculated using (7), and can be applied to modeling the channel. Similar to the oxygen absorption loss, rain attenuation can be applied to the cluster responses:

$$AL_n(f_c) = \frac{A_r(f_c)}{1000}(d + c(\tau_n + \tau_\Delta)) \qquad \text{(dB)} \qquad (9)$$

where $A_r(f_c)$ (dB/km) is rain induced signal attenuation that can be calculated based on (7). c (m/s) is the speed of light, and d (m) is the separation distance between the transmitter and receiver distance. τ_n(s) is the n-th cluster delay, τ_Δ is 0 in the LOS case, and minimum delay min $(\tau_\Delta^{'})$ otherwise [20]. The final frequency-domain channel response is obtained by the summation of frequency-domain channel responses of all clusters. Time-domain channel response is obtained by the reverse transform from the obtained frequency domain channel response.

In the next section, we will focus on the impacts of rain on millimeter-wave signal, and takes the rain attenuation into consideration for 5G simulation using the measured monitored signal-to-noise ratio.

III. EXPERIMENTAL SETUP

A. MILLIMETER-WAVE LINK MEASUREMENT SETUP

As shown in Fig. 7, we carried out millimeter-wave link measurement at Institute of Atmospheric Physics, Chinese Academy of Sciences in central Beijing, China in 2017 and April 2018. The schematic diagram of transmission link in dry and rainy weather is illustrated in Fig. 1. For our measurements, we selected 23 GHz, 25 GHz, 28 GHz, and 38 GHz to be the link frequencies. These frequencies in millimeter frequency band have been recognized by cellular industry for future wireless technologies [35]–[37]. The 28 GHz and 38 GHz bands are also licensed for wireless backhaul communications [39]. The link length was 0.7 km. The link budget for the measurements are given in Table 2.

For the transmit side, an Anritsu MG369XB series signal generator is used to produce any signal up to 40 GHz. The output signal is connected to a vertical polarized horn antenna, and its gain is given in Table 2. The transmit signal stability is monitored using a Rohde & Schwarz power meter. The transmitter produces a stable transmit power with negligible temperature induced variations.

The receiver setup consists of a vertically polarized horn antenna, and the signal reception is carried out using an Agilent N9030A PXA signal analyzer up to 40 GHz. At the receiver side, we developed a software program to monitor the instantaneous received signal level, and recorded the data every 15 s. LOS route was investigated. The horn antenna at transmit and receive side are identical. A total

TABLE 2. Beijing measurement link budgets.

Parameter	23 GHz (2017)	25 GHz (2017)	28 GHz (2017)	38 GHz (2017-18)
Frequency	23 GHz	25 GHz	28 GHz	38 GHz
Tx power	7 dBm	7 dBm	7 dBm	7 dBm
Antenna type	Horn antenna, VSWR≤1.5			
Tx antenna gain	25.1 dBi	23.765 dBi	24.4 dBi	25.6 dBi
EIRP	32.1 dBm	30.765 dBm	31.4 dBm	32.6 dBm
Tx AZ. HPBW	9.6°	11°	10.4°	8.4°
Tx EL. HPBW	8.5°	10°	9.4°	7.4°
Tx polarization	V	V	V	V
Tx cable loss	-2.23 dB	-2.23 dB	-2.23 dB	-2.23 dB
Rx antenna gain	25.1 dBi	23.765 dBi	24.4 dBi	25.6 dBi
Rx AZ. HPBW	9.6°	11°	10.4°	8.4°
Rx EL. HPBW	8.5°	10°	9.4°	7.4°
Rx polarization	V	V	V	V
Rx cable loss	-4.95 dB	-4.95 dB	-4.95 dB	-4.95 dB
Tx-Rx distance	700 m	700 m	700 m	700 m
FSPL (n=2)	116.54	117.26 dB	118.25 dB	120.90 dB
Theoretical Rx power (n=2)	-66.5 dBm	-69.9 dBm	-69.6 dBm	-69.8 dBm
Rx sensitivity	-100 dBm	-100 dBm	-100 dBm	-100 dBm
Fade margin	33.5 dB	30.1 dB	30.4 dB	30.1 dB

FIGURE 7. Millimeter-wave transmission link at Institute of Atmospheric Physics, Chinese Academy of Sciences, Beijing, China.

TABLE 3. Measurements records.

Link freq	Rain time	Peak rain rate	Length	Location
23 GHz	1633 mins	17.9 mm/h	0.7 km	Beijing
25 GHz	528 mins	118.0 mm/h	0.7 km	Beijing
28 GHz	257 mins	7.2 mm/h	0.7 km	Beijing
38 GHz	1640 mins	16.3 mm/h	0.7 km	Beijing
72.625 GHz/ 82.625 GHz	1025 mins	12.6 mm/h	3 km	Göteborg

of 28,800 received signal level samples were recorded during the measurement in 2017.

The rain induced signal attenuation is compared with measurements from two rain disdrometers and one rain gauge in the test area. Those rainfall monitoring equipments have been calibrated to take one measurement every minute. A total of 63.5 rain hours were recorded in 2017 as listed in Table 3.

For LOS link, the channel is expected to follow Rician fading distribution, which can be expressed as:

$$f_X(x) = \frac{x}{\sigma^2}\exp\left(-\frac{(x^2+A^2)}{2\sigma^2}\right) I_0\left(\frac{Ax}{\sigma^2}\right) \qquad (10)$$

$$K = \frac{A^2}{2\sigma^2}$$

where $I_0(\cdot)$ is the modified Bessel function of the first kind and zero order, A is the amplitude of the dominant signal, and σ is the standard deviation of all other weak signals. The parameter K is the Rician factor and specifies the Rician distribution.

To better understand our measurement environment and channel characteristics in Beijing, we examined our measurement results during dry time before rain. The cumulative distribution function (CDF) functions for the received signal level relative to its mean value for the measurements are plotted in Fig. 8. For comparison, the CDF of a Rayleigh distribution, and Rician distribution with various K-factors in increments of 5 dB are also plotted. The empirical results show that for our measurements, the Rician distribution gives the best fit to the data.

B. E-BAND MEASUREMENT

In order to study the impact of rain on E-band millimeter-wave links, we obtained the commercial millimeter-wave backhaul link measurement data provided by Ericsson. The measurement was conducted in Göteborg, Sweden, and microwave equipment was installed at two sites, site A in Lindholmen (57° 42′ 18.97″ N, 11° 56′ 29.67″E) and site B in Älvsborgsbron (57°41′20.04″N, 11°54′10.76″E). There are two links installed between Site A and Site B, and link A was operated at a frequency of 72.625 GHz using vertical polarization with a transmit power at 8 dBm. Link B was operated at a frequency of 82.625 GHz using vertical polarization with a transmit power at 9.5 dBm. The antenna gains at both sites are 50.5 dBi. Both links were 3 km long, and the received signal level was recorded at 30-seconds intervals. Rain, humidity, temperature, air pressure and wind information was provided by a weather station near the site B, located at the rooftop of Ericsson building. The measurement period was between 7 June to 17 June 2017.

C. MEASUREMENT DATA PROCESSING

Based on the rain rate measurement recorded by the disdrometer and rain gauge, the rain induced attenuation can be calculated based on ITU equation (7). The coefficients a and b in equation (7) can be calculated using the following equations:

$$a = \left(a_H + a_V + (a_H + a_V)\cos^2\theta\cos 2\tau\right)/2 \qquad (11)$$

$$b = \left(a_H b_H + a_V b_V + (a_H b_H - a_V b_V)\cos^2\theta\cos 2\tau\right)/2a$$

where θ is the path elevation angle, and τ is the polarization tilt angle relative to the horizontal. In our measurements, both the transmit and receive antenna are vertically polarized, and the resulting power-law coefficients are given in Table 4.

The measured rain-induced attenuation (A_r) is calculated by subtracting the received signal level from the

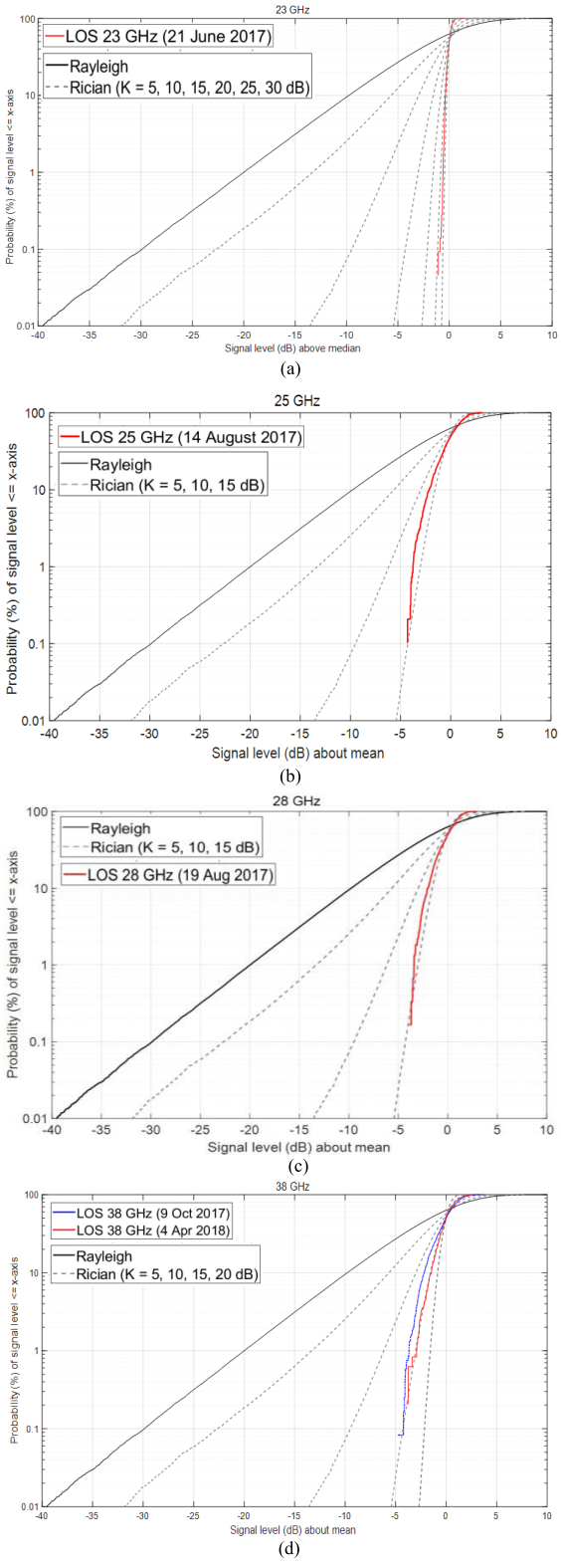

FIGURE 8. CDF plot of the received signal power relative to the mean value for the (a) 23 GHz link on 21 June 2017. (b) 25 GHz link on 14 August 2017. (c) 28 GHz link on 19 August 2017. (d) 38 GHz link on 9 Oct 2017 and 4 Apr 2018. Rayleigh and Rician distributions (K factors range from 5 dB to 30 dB) are also plotted for comparison.

TABLE 4. Link budgets power law coefficients for different frequencies.

Frequency	a_H	a_V	b_H	b_V	a	b
23 GHz	0.1286	0.1284	1.0214	0.9630	0.1284	0.9630
25 GHz	0.1571	0.1533	0.9991	0.9491	0.1533	0.9491
28 GHz	0.2051	0.1964	0.9679	0.9277	0.1964	0.9277
38 GHz	0.4001	0.3844	0.8816	0.8552	0.3844	0.8552
73 GHz	1.0764	1.0711	0.7268	0.7150	1.0711	0.7150
83 GHz	1.2063	1.2034	0.7058	0.6973	1.2034	0.6973

millimeter-wave link in rainy period from the average received signal level in dry period. During the experiment in Beijing, we are able to record the received signal strength every 15s. For the E-band experiment in Göteborg, the sampling interval is 30 seconds. The received signal attenuation measurement vector is expressed as $\boldsymbol{A_r} = [A_{r,1}, A_{r,2}, A_{r,3}, \ldots, A_{r,N}]^T$, and all the elements are sampled at constant intervals. The rain rate measurement vector is $\boldsymbol{R} = [R_1, R_2, R_3, \ldots, R_M]^T$, which entries are sampled at constant intervals of 1 min. The measured signal attenuation are grouped and the average of the signal attenuation is computed every 1 minute: the number of instantaneous received signal attenuation observations during every 1-minute measurement is $K = 4$ (15s sampling interval) or $K = 2$ (30s sampling interval). For the same period of time, the number of instantaneous rain rate measurements is $S = 1$.

Therefore, for comparison studies, from N original signal attenuation observations and M original rain rate observations, $I = N/K = M/S$ groups of samples are available. Since $S = 1$, therefore $I = M$. Based on (7), for the i^{th} rain rate sample, the theoretical rain induced attenuation for the given rain rate is:

$$A_{link-avg,i} = \frac{\sum_{j=1}^{K} \left(A_{r,Ki+j}\right)}{K} (\text{mm/h}) \tag{12}$$

where R_i (mm/h) is the measured rain rate during the i^{th} time interval. For i^{th} group of signal attenuation samples, the average signal attenuation from the millimeter-wave link can be derived as:

$$A_{cal,i} = aR_i^b (\text{mm/h}) \tag{13}$$

The average rain induced signal attenuation from the measurement $A_{link-avg,i}$ is compared with the $A_{cal,i}$ in the following sections.

D. MEASUREMENT RESULTS

1) 23 GHZ

Fig. 9a and 9b present the variations of the received signal strength and rain intensity measurement obtained from the 23 GHz wireless link on 22, June 2017. The average rain intensity was 1 mm/h, and highest rain intensity was 7 mm/h. The signal was affected by the rain, and attenuated. The rain lasted for around 5 hours. When the rain just started,

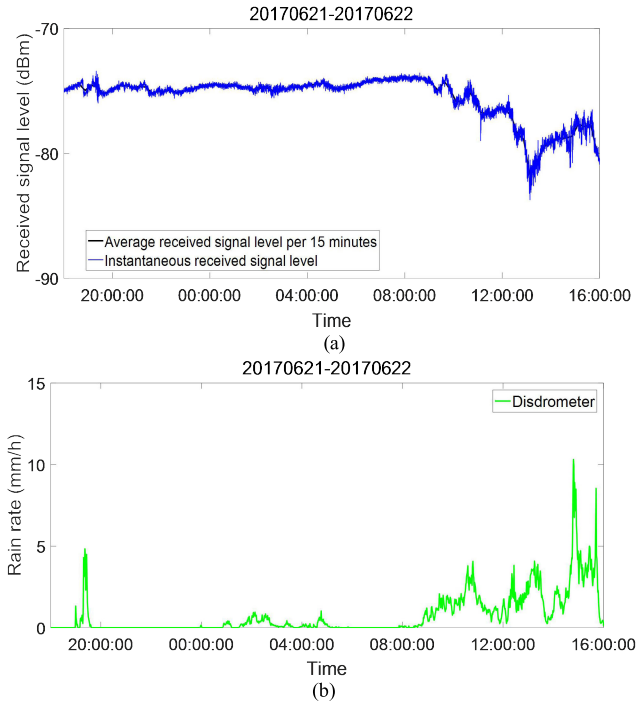

FIGURE 9. (a) The rain rate measurement on 22 June 2017 (b) The rain induced signal attenuation on 22 June 2017.

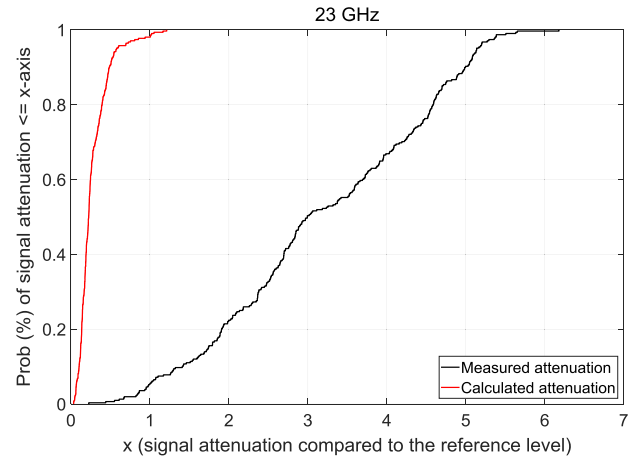

FIGURE 10. CDF plot of the calculated and measured signal attenuation due to rain for the 23 GHz LOS millimeter-wave link measurement.

the signal attenuation was between 1 – 2 dB, and became 1.5 – 3.5 dB after 1 hour, and increased to 2.5 – 5.5 dB after 2.5 hours. As the rain continued dampening the antenna, the additional signal loss was mainly due to the wetness of the antenna surface, and the attenuation became higher as the antenna became more wet. Since 23 GHz was near the absorption peak frequency of 22.235 GHz for water vapour, the signal attenuation due to water vapour contributed to 0.5 dB signal attenuation during the measurement period in addition to rain induced attenuation. The difference between the measured signal attenuation and calculated attenuation using (7) was presented in Fig. 10, and the difference was up to 4.3 dB mainly due to wet antenna and water vapour.

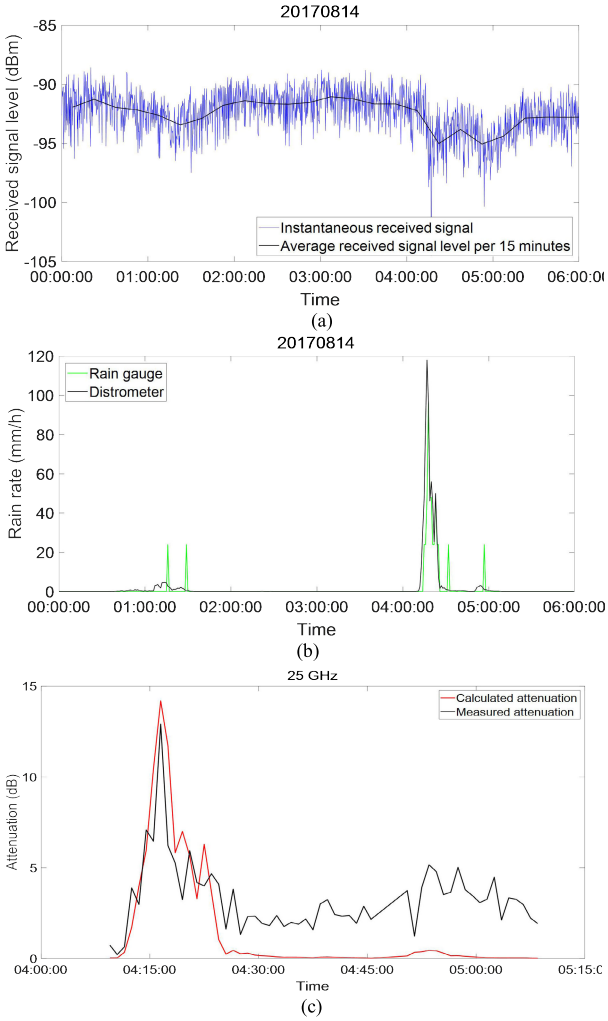

FIGURE 11. (a) The received signal variation of 25 GHz link on 14 August 2017. (b) Rain rate measurement. (c) Comparison between calculated the attenuation based on ITU model and measured attenuation.

2) 25 GHZ

Fig. 11a and 11b presents the measured signal attenuation of the 25 GHz wireless link and instantaneous rain rate on 14 August 2017. The signal was clearly affected by the rain. Extreme heavy rain happened, and the peak rain intensity reached 118 mm/h, and the average rain intensity was 8 mm/h. During the extreme heavy rain time, the calculated attenuation using ITU model and rain rate measurement appeared to be higher than the measured attenuation from the link as indicated in Fig. 11c. The reason was that the received signal level of the link was reduced below the noise level and could not be detected when the rain was over 80 mm/h, and therefore the rain induced attenuation could not be retrieved. As the rain intensity reduced, the calculated signal attenuation became less than the measured attenuation. As shown in Fig. 12, the CDF plot of the calculated and measured attenuation during 13-14 August 2017, apart from the extremely heavy rain time, at around 90% of the time, the calculated signal attenuation was less

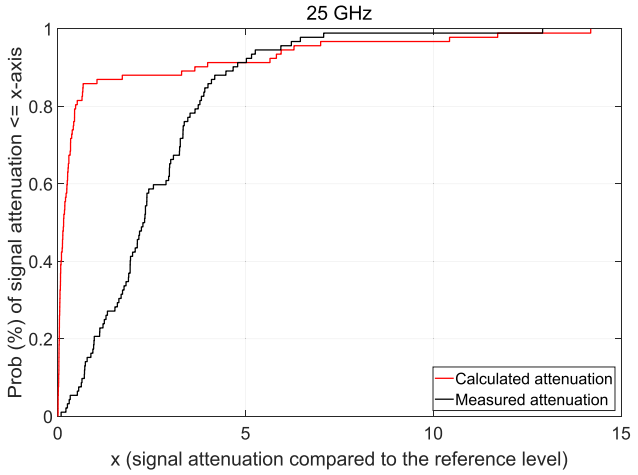

FIGURE 12. CDF plot of the calculated and measured signal attenuation due to rain for the 25 GHz LOS millimeter-wave link measurement.

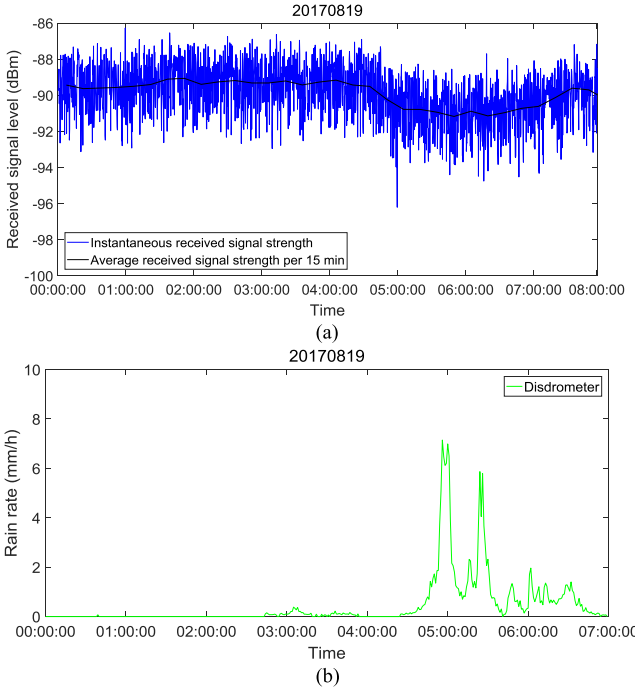

FIGURE 13. (a) The received signal strength on 19 August 2017. (b) The disdrometer and rain gauge measurement nearby.

than 3 dB, compared to the observed signal attenuation of 1 - 5 dB. The signal was attenuated by approximately 2 dB, mainly due to water on the antenna.

3) 28 GHZ

Fig. 13 shows the measurement at 28 GHz on 19 August 2017. For the 28 GHz link, the average and peak rain intensity was 0.7 mm/h and 7 mm/h on 19 August 2017. The calculated signal attenuation was approximately 1 dB, and the average observed signal attenuation was between 1 dB to 2.5 dB for a rain rate of 0 - 7 mm/h, as shown in Fig. 14.

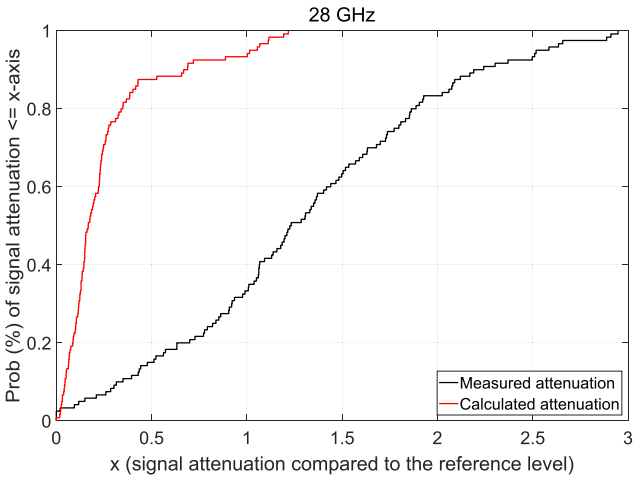

FIGURE 14. CDF plot of the calculated and measured signal attenuation due to rain for the 28 GHz LOS millimeter-wave link measurement.

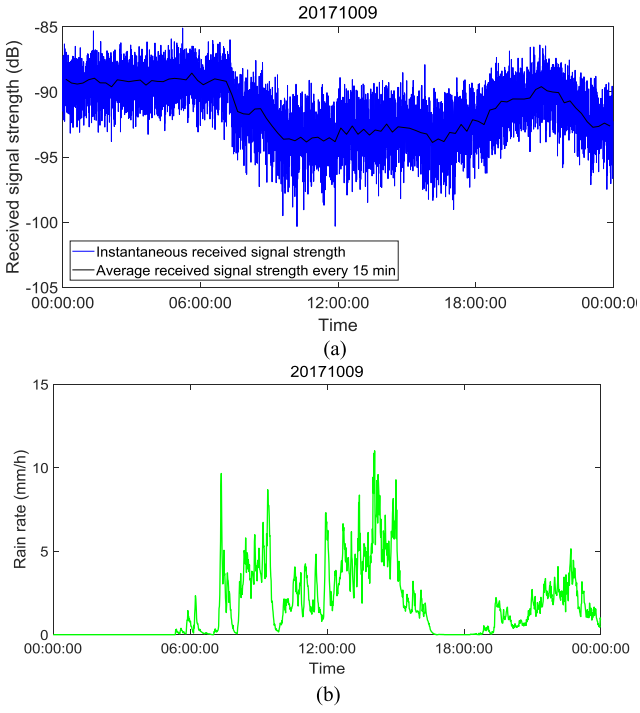

FIGURE 15. (a) The received signal strength attenuation on 9 Oct 2017. (b) The disdrometer measurement nearby.

4) 38 GHZ

On 9 Oct 2017, the link frequency was increased to 38 GHz. The average rain intensity during the day was 2.2 mm/h, and the peak rain rate was 11 mm/h. The calculated signal attenuation due to the rain and water vapour was approximately 2.5 dB. The observed received signal attenuation was between 1 - 6 dB, as shown in Fig. 15. We also carried out a 38 GHz link measurement on 4 April 2018. The average rain intensity was 2 mm/h, and the peak rain intensity was 17 mm/h. The link measurement showed that signal experienced deep fades during rain, attenuated by 1-6 dB, while the calculated signal attenuation using ITU model was up to 3 dB, and the difference is compared in Fig. 16.

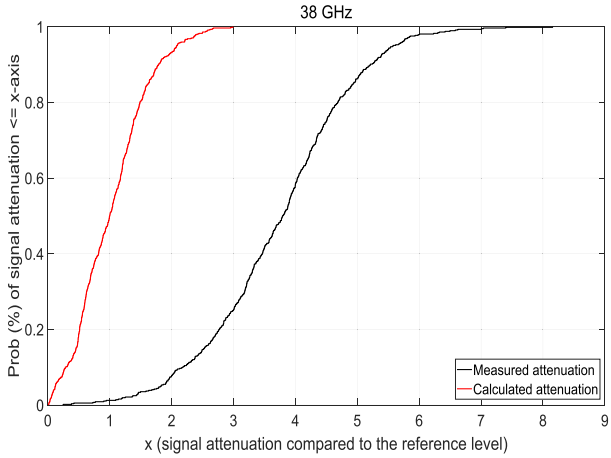

FIGURE 16. CDF plot of the calculated and measured signal attenuation due to rain for the 38 GHz LOS millimeter-wave link measurement.

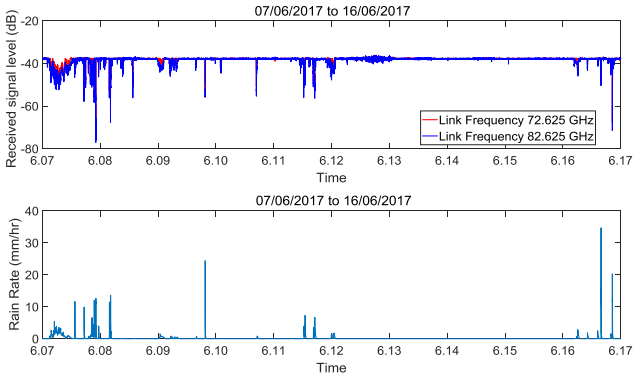

FIGURE 17. Received signal level of 72.625 GHz and 82.625 GHz link affected by the rain between 7 June and 17 June 2017.

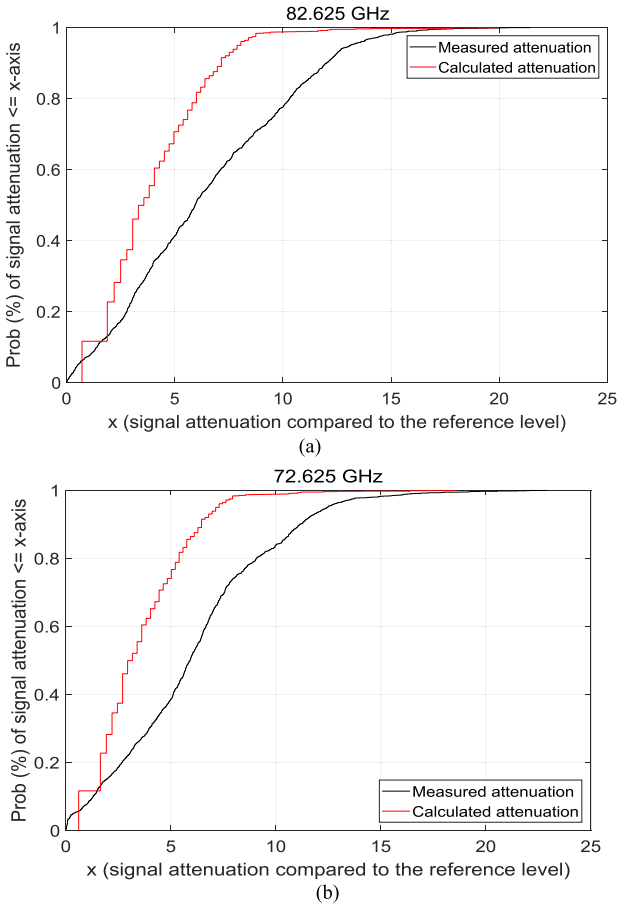

FIGURE 18. CDF plot of the calculated and measured signal attenuation due to rain for the (a) 72.625 GHz link measurement, (b) 82.625 GHz link measurement.

The attenuation of microwave signal depends on the rain intensity as well as the droplet size both. The total extinction cross section for typical rain is more for 38 GHz than signals at lower frequencies, causing more attenuation at 38 GHz.

5) E-BAND

The E-band link A at 72.625 GHz and link B at 82.625 GHz were in operation at the same time. During the measurement period, rain events occurred in 5 out of 11 days.

The variation of the receive signal level of both links are presented together with the rain intensity over the measurement period in Fig. 17. As expected, power attenuation is mainly due to rainfall, and they are highly correlated resulting in a correlation coefficient of 0.8. For the experiment period, the CDF plot of the calculated and measured attenuation during rain was compared in Fig. 18. For the 72.625 GHz link, the observed signal attenuation reached 20 dB, and uncertainties caused up to 4 dB additional attenuation compared to calculated attenuation values. The attenuation for 82.625 GHz link was even higher. The observed signal attenuation reached 22 dB, and additional attenuation due to uncertainties was up to 4.5 dB.

Table 5 summaries the theoretical and measured signal attenuation for the different rain events. Although it is not meaningful to directly compare the attenuation values as the rain rate varies from time to time, it is noticed that the measured attenuation is greater than the theoretical signal attenuation by 1.5 - 4.5 dB, mainly due to humidity, wet antenna. Humidity can contribute over 0.6 dB/km for E-band signals. For a rainfall event lasting for a long period of time, the wet antenna attenuation is expected to increase with increasing thickness of water film on the antenna, [17], [39]. For high frequencies, wet antenna attenuation can be high even for low rain rates [40]. The disdrometer provides a point

TABLE 5. Attenuation summary.

Frequency	Calculated signal attenuation	Measured attenuation	Uncertainty
23 GHz	⩽1.2 dB	⩽5.5 dB	4.3 dB
25 GHz	⩽ 14 dB (extreme heavy rain) ⩽3 dB	⩽ 13 dB ⩽5 dB	2.0 dB
28 GHz	⩽1.5 dB	⩽3 dB	1.5 dB
38 GHz	⩽3 dB	⩽ 6dB	3.0 dB
72.625GHz	⩽18	⩽20	4.0 dB
82.625GHz	⩽20	⩽22	4.5 dB

TABLE 6. Parameters for the considered OFDM system.

Parameter		Value
Waveform		OFDM
Multiplexing		TDD
Center frequency		23 GHz
Frame length		10 ms
Sub-frame length		1 ms (10 sub-frames per frame)
Sub-carrier spacing		15 kHz
Number of slots		2 slots per sub-frame
Sampling rate		30.72 MHz
Sampling time		32.55 ns
Number of OFDM symbols		14 with normal cyclic prefix
OFDM symbol duration		66.67 μs
Cyclic prefix length	short	(5.2 μs/160 samples) x 1 symbol
		(4.7 μs/144 samples) x 6 symbols
	long	(16.7 μs/512 samples)
Bandwidth		20 MHz
Number of FFT		2048
Sub-carrier spacing		15 kHz
Resource block size		12 sub-carriers per resource block
Number of resource blocks		100
Coding		LDPC
Modulation and coding scheme		QPSK 1/3, QPSK 1/2, 16 QAM 1/2, 16 QAM 3/4, 64 QAM 2/3, 64 QAM 5/6, 256 QAM 3/4, 256 QAM 5/6

measurement, while the signal attenuation is caused by the rain along the link, rain intensity could vary and be different from the disdrometer measurement and could also contribute to the difference in attenuation value. The experiment in Beijing was conducted using signal generator and spectrum analyzer, both were calibrated to be able to maintain stable signal transmission and reception. However, for commercial microwave backhaul links, the stability of the transmit power are not as good as the lab instruments, and bias could be up to 1.6 dB [38], therefore causing more attenuation to the received signal level.

IV. PROPOSED RAIN-AWARE LINK ADAPTATION ALGORITHM AND SIMULATION RESULTS

A. 5G SIMULATION ASSUMPTIONS

We consider an OFDM (orthogonal frequency division multiplexing) based 5G millimeter-wave downlink transmission. The parameters are summarized as below in Table 6. A representative sample of the modulation and coding schemes (MCSs) adopted by the latest 3GPP standards are used, indicated in Table 7 [41]. The effective data rate of a MCS is R = (number of data subcarriers per symbol × coding rate × number of coded bits per symbol × number of OFDM symbols per time slot)/duration of time slot. The spectral efficiency for different schemes is also given in Table 7. The 5G millimeter-wave simulation is evaluated using the LOS urban micro propagation model defined in 3GPP TR 38.901 [32]. Clustered delay line D model (CDL-D) is used for simulation.

TABLE 7. Modulation and coding schemes.

MCS	Modulation	Coded bits per symbol	Coding rate	Bit rate R Mbps	Spectral efficiency bps/Hz
1	QPSK	2	1/3	8.76	0.438
2	QPSK	2	1/2	12.22	0.611
3	16 QAM	4	1/2	25.46	1.273
4	16 QAM	4	3/4	30.58	1.529
5	64 QAM	6	2/3	50.61	3.083
6	64 QAM	6	5/6	61.66	3.078
7	256 QAM	8	3/4	73.71	3.666
8	256 QAM	8	5/6	84.04	4.202

B. DYNAMIC RAIN-AWARE RADIO RESOURCE MANAGEMENT ALGORITHM

Link adaptation (LA), as one of the radio resource management (RRM) schemes, denotes the matching of modulation, coding and signal parameters to the conditions of radio link. It can be seen from section III that the received signal power varies due to changing channel conditions. The resulted signal-to-noise ratio (SNR) at the receiver also varies. If the transmission parameters were set to deal with the worst case channel condition, a lot of capacity would be wasted when the signal link experiences good channel conditions. Here we consider an adaptive modulation and coding LA scheme, and the transmission parameters are continuously adjusted to the channel conditions to enable transmission for the given received SNR.

Assuming the prediction of local weather information is available (e.g. rain intensity R can be derived from the radar reflectivity of rain [42]–[44]), the additional signal attenuation due to the rain A_r can be estimated using equation (7). Based on the location information, channel information of a mobile terminal, the local atmospheric condition, the resulted instantaneous received SNR is expressed as:

$$SNR = \frac{P_R}{N_0 B} = \frac{P_R}{N} \tag{14}$$

where N_0 is the noise power density, N is the noise power for the given bandwidth B. We consider 9 different combinations of MCS given in Table 7. For a given MCS, the achievable link throughput T_m is:

$$T_m = R_m\,(1 - BLER_m) \tag{15}$$

where R_m and $BLER_m$ are the data rate and the block error rate ($BLER$) of m_{th} MCS scheme. $BLER$a ratio of the number of erroneous blocks to the total number of blocks transmitted. For the MCS with index m, the maximum achievable throughput T_m and the received SNR requirements γ_m for each MCS scheme can be obtained from Fig. 19. A certain quality of service (QoS) is usually imposed, and the $BLER$ needs to be no more than the target block error rate ($BLER_{target}$) (1%).

A dynamic rain-aware link adaptation algorithm (R-LA) is proposed here. It is based on a greedy approach, and its objective is to select the MCS scheme with the maximum

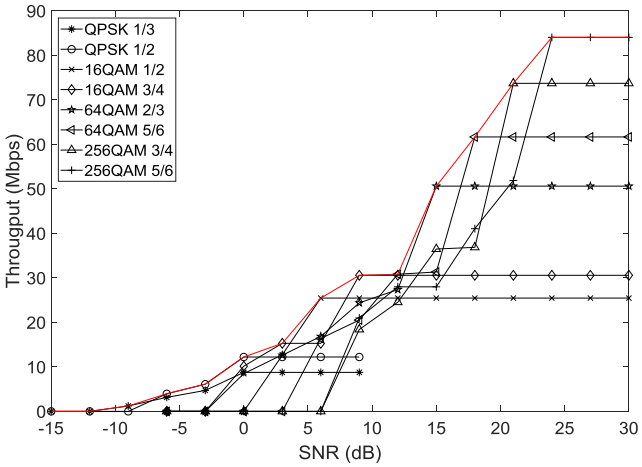

FIGURE 19. Simulated OFDM link throughput for all the considered MCSs.

throughput for the given received SNR level while meeting the *BLER* constraint $BLER_{target}$,

$$\begin{aligned} &\max R_m\,(1 - BLER_m) \\ &\text{s.t. } C1: BLER_m \le BLER_{\text{target}} \\ &\quad C2: SNR = \gamma_m \\ &\quad C3: m \in \mathbf{M} \\ &\quad C4: P_R > \text{receiver sensitivity} \end{aligned} \tag{16}$$

$\mathbf{M}$ is the set of all possible MCSs, $\mathbf{M} = \{1, 2, 3, \ldots, M.\}$

C. PERFORMANCE EVALUATION

Here we consider the rainfall event on 21-22 June 2017 for illustrating our proposed R-LA scheme. The received SNR of the signal link between 6 pm on 21 June and 4 pm on 22 June can be calculated using equation (14) based on the measurements presented in Fig. 9. For rain detection and observation, it has been shown that X-band radars can be an effective

Algorithm Dynamic Rain-Aware Link Adaptation Algorithm (R-LA)

1: Based on the location of the transmitter and receiver, obtain the local rain intensity information R, compute the atmospheric attenuation value aR^b
2: Compute the effective *SNR*
3: Compute the throughput of MCS mode 1 as the LA throughput performance threshold $T_{threshold} = R_1$ (1-$BLER_1$)
4: $M = 8$
5: **for** $m = 2$ to M **do**
6: Compute the link throughput T_m according to (12);
7: **if** $T_m > T_{threshold}$ **then**
8: Select MCS mode m as transmission mode
9: **else**
10: Select MCS mode 1 as transmission mode
11: **end if**
12: **end for**
13: Save the index of the selected MCS mode. This will need to be fed back to the transmitter for adaptation.

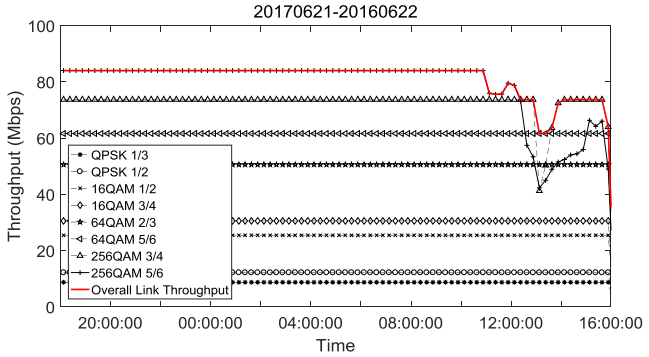

FIGURE 20. The link throughput of different MCSs and R-LA on 21–22 June 2017.

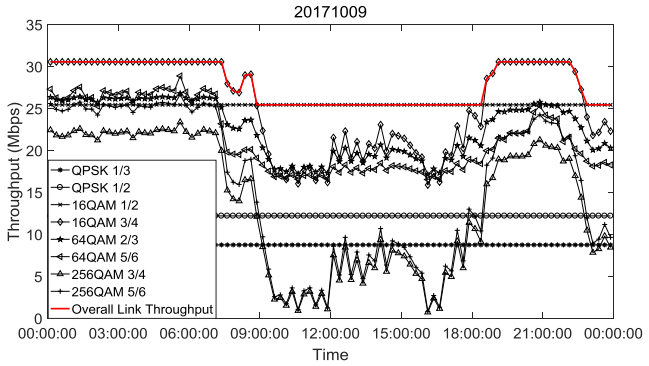

FIGURE 21. The link throughput of different MCSs and R-LA on 9 Oct 2017.

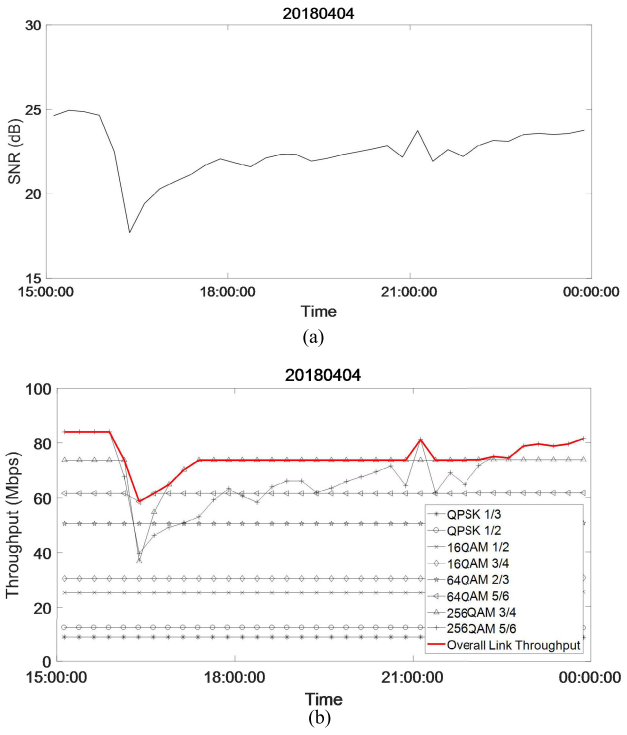

FIGURE 22. (a) The received signal-to-noise variation on 4 April 2018. (b) The link throughput of different MCSs and R-LA.

tool for high temporal and spatial resolution rainfall parameter retrievals. The microwave and remote sensing group from IAP analyzed an overall of 1650 copies of disdrometer

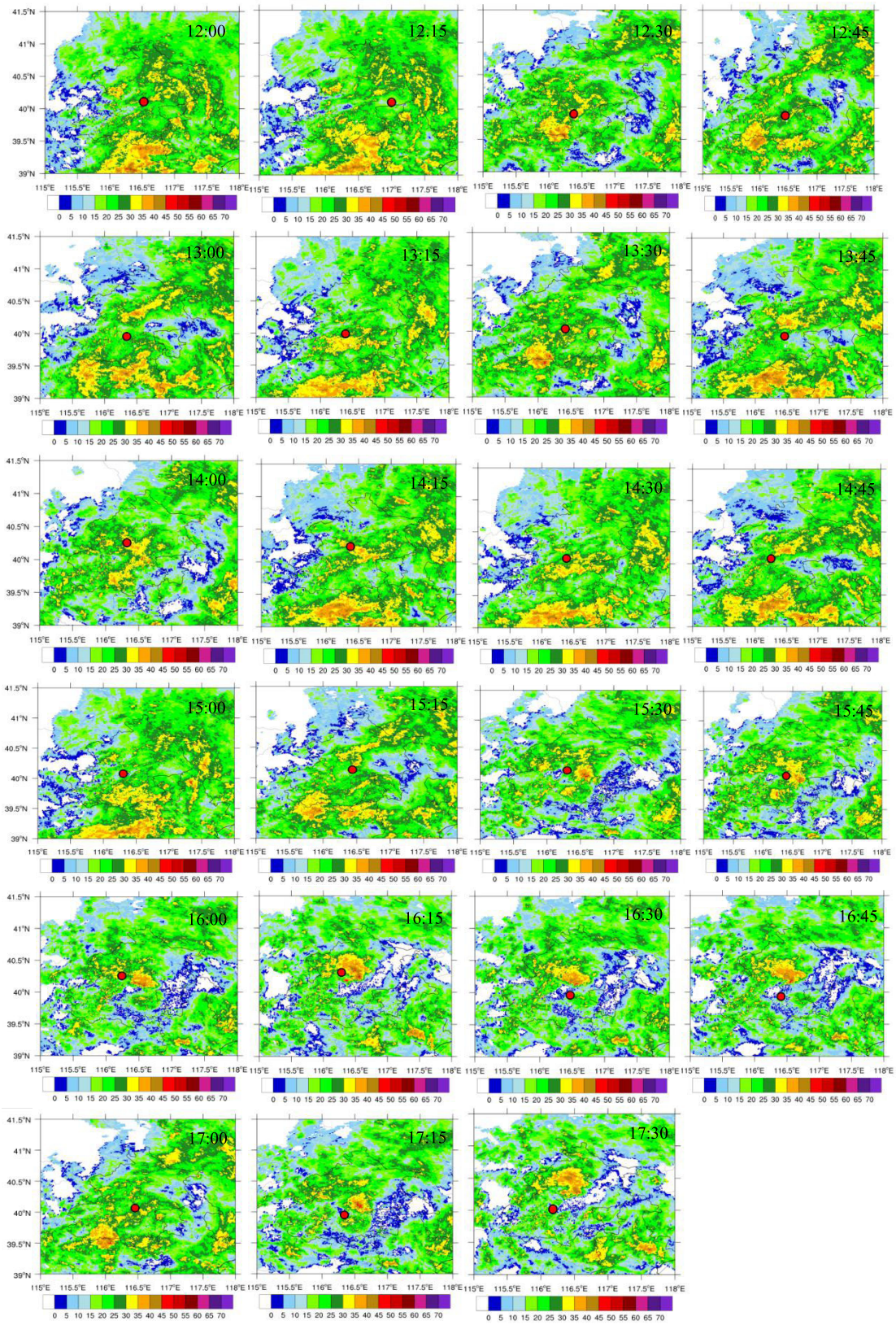

FIGURE 23. The time series of radar reflectivity on 22 June 2017 between 12–5.30 pm (the colour bar shows the reflectivity value).

measurement data which was collected in Beijing for many years, and based on the statistical analysis and calculations, worked out the relationship between rain rate R and radar reflectivity Z for X-band radar to be [45]:

$$Z = 237R^{1.57} \tag{17}$$

The time series of X-band dual-polarization weather radar reflectivity between 12 pm and 5.30 pm on 22 June 2017 are plotted in Fig. 23 provided by the Beijing Meteorological Services. The rain intensity can be retrieved from radar reflectivity data using equation (17), and rainfall events can be predicted by monitoring the changes of radar reflectivity plots.

Assuming the information on rain intensity prediction is available, the link throughput of an OFDM system employing different MCSs is compared to the same system adopting the R-LA scheme. It is shown in Fig. 20 that the R-LA scheme allows the system to adapt to the changing weather condition better, and giving the best throughput, while the throughput for fixed modulation and coding scheme is between 12% to 93% of the system employing R-LA scheme.

We also examined the R-LA algorithm using the 38 GHz link measurement on 9 Oct 2017 and 4 April 2018. The variations of received SNR and link throughput results are presented in Fig. 21 and Fig. 22. For the rainfall event on 9 Oct 2017, the link throughput of system employing an individual MCS is between 12% to 93% of the system employing R-LA scheme. For the measurement on 4 April 2018, the R-LA scheme also shows the best performance and the link throughput for a fixed modulation and coding scheme is 5% - 88% less compared to a R-LA based system.

Here we assume a single user scenario, the algorithm can be extended to a multi-user scenario.

V. CONCLUSIONS

Millimeter frequency band is expected to be used widely for both wireless backhaul links and also data transmission links in the near future. Since rain, humidity and other weather factors affect the attenuation of signal, it is important to consider it for channel modeling and wireless link performance evaluation.

For heavy rain, as frequency increases from 28 GHz to 73 GHz, the signal experiences 9 - 19 dB attenuation. High humid level can increase the signal attenuation by 0.15 dB/km - 0.45 dB/km for signals at the frequency range of 28 GHz - 78 GHz. Heavy fog may cause signal attenuation from 0.23 dB/km up to 1.34 dB/km for wireless links between 28 GHz and 78 GHz.

We carried out millimeter-wave propagation measurement in Beijing, China. We tested along a 0.7 km long signal link as examples of LOS transmission links, which could also represent a millimeter-wave backhaul link. We also studied a 3 km long commercial millimeter-wave backhaul link at 72.625 GHz and 82.625 GHz in Göteborg, Sweden. We focused on the impacts of rain on signal link quality. From measurements results we could see the propagating signal attenuate as a result of changing weather conditions. By comparing the signal attenuation calculated from empirical equation and real-time measurement, it was shown that in addition to the ITU power-law equation for estimating the rain induced signal attenuation, other factors such as wet antenna effect, change of humidity level, and equipment stability may also impact the signal attenuation in practice. The outdoor measurements showed these uncertainties could cause signal attenuation between 1.5 - 4.5 dB. Based on the assumption of rain prediction and real time rain monitoring, a dynamic rain-aware link adaptation scheme is proposed to allow the system to adapt the modulation and coding scheme to rain intensity levels, and outperform system employing fixed modulation and coding schemes. Severe rainfall events happen more often in Southern China and the rainy season there is longer compared to Beijing. We will continue our measurements in Beijing and cities in South China, and will examine different link lengths in the near future.

ACKNOWLEDGMENT

The authors would like to thank Prof. Hagit Messer, Prof. Hui Xiao for their helpful discussions. They would like to thank Ericsson for giving them access to data. They would also like to thank Dr. Lei Bao at Ericsson Research.

REFERENCES

[1] R. C. Daniels, R. W. Heath, J. N. Murdock, T. S. Rappaport, *Millimeter Wave Wireless Communications: Systems and Circuits*. Upper Saddle River, NJ, USA: Prentice Hall, Sep. 2014.

[2] H. Zhang, S. Huang, C. Jiang, K. Long, V. C. M. Leung, and H. V. Poor, "Energy efficient user association and power allocation in millimeter-wave-based ultra dense networks with energy harvesting base stations," *IEEE J. Sel. Areas Commun.*, vol. 35, no. 9, pp. 1936–1947, Sep. 2017.

[3] A. L. Swindlehurst, E. Ayanoglu, P. Heydari, and F. Capolino, "Millimeter-wave massive MIMO: The next wireless revolution?" *IEEE Commun. Mag.*, vol. 52, no. 9, pp. 56–62, Sep. 2014.

[4] *Studies on Frequency-Related Matters for International Mobile Telecommunications Identification Including Possible Additional Allocations to the Mobile Services on a Primary Basis in Portion(s) of the Frequency Range Between 24.25 and 86GHz for the Future Development of International Mobile Telecommunications for 2020 and Beyond*, document 238 WRC-15, 2018. [Online]. Available: https://www.itu.int/dms_pub/itu-r/oth/0c/0a/R0C0A0000 0C0014PDFE.pdf

[5] *Agenda and Reference (Resolutions and Recommendations)*, ITU, Geneva, Switzerland, Aug. 2017. [Online]. Available: https://www.itu.int/dms_pub/itu-r/oth/14/02/R14020000 010001PDFE.pdf

[6] C. Sacchi, T. Rahman, I. A. Hemadeh, and M. El-Hajjar, "Millimeter-wave transmission for small-cell backhaul in dense urban environment: A solution based on MIMO-OFDM and space-time shift keying (STSK)," *IEEE Access*, vol. 5, pp. 4000–4017, 2017.

[7] (2018). *Ericsson Mobility Report*. [Online]. Available: https://www.ericsson.com/assets/local/microwave-outlook/documents/ericsson-microwave-outlook-report-2018.pdf

[8] *Frequency Band Review for Fixed Wireless Services*, document 2315/FLBR/FRP/3, Nov. 2011. [Online]. Available: http://stakeholders.ofcom.org.uk/binaries/consultations/spectrum-review/annexes/report.pdf

[9] J. Karjalainen, M. Nekovee, H. Benn, W. Kim, J. Park, and H. Sunsoo, "Challenges and opportunities of mm-wave communication in 5G networks," in *Proc. Int. Conf. Cogn. Radio Oriented Wireless Netw. Commun. (CROWNCOM)*, Jun. 2014, pp. 372–376.

[10] Y. Niu, Y. Li, D. Jin, L. Su, and A. V. Vasilakos, "A survey of millimeter wave communications (mmWave) for 5G: Opportunities and challenges," *Wireless Netw.*, vol. 21, no. 8, pp. 2657–2676, Nov. 2015.

[11] T. Wang and B. Huang, "Millimeter-wave techniques for 5G mobile communications systems: Challenges, framework and way forward," in *Proc. URSI GASS*, Aug. 2014, pp. 1–4.

[12] T. S. Rappaport, Y. Xing, G. R. MacCarney, A. F. Molisch, E. Mellios, and J. Zhang, "Overview of millimeter wave communications for fifth-generation (5G) wireless networksâĂŤwith a focus on propagation models," *IEEE Trans. Antennas Propag.*, vol. 65, no. 12, pp. 6213–6230, Dec. 2017.

[13] M. Coldrey *et al.*, "Maturity and field proven experience of millimeter wave transmission," ETSI, White Paper 10, Sep. 2015, pp. 1–61. [Online]. Available: https://www.etsi.org/images/files/ETSIWhitePapers/etsi_wp10_field_proven_experience_of_mwt_20150923.pdf

[14] D. Atlas and C. W. Ulbrich, "Path-and area-integrated rainfall measurement by microwave attenuation in the 1–3 cm band," *J. Appl. Meteorol.*, vol. 16, no. 11, pp. 1322–1331, 1977.

[15] Q. Zhao and J. Li, "Rain attenuation in millimeter wave ranges," in *Proc. Int. Symp. Antennas, Propag., EM Theory*, Oct. 2006, pp. 1–4.

[16] T. Hirano , T. Sugiyama, J. Hirokawa, M. Ando, H. Nagahori, K. Saito, T. Taniguchi, Y. Koyama , and I. Kurosawa, "Development of Tokyo Tech Ookayama campus millimeter-wave model network and propagation characteristics in 25GHz band," *IEICE Tech. Rep. Antennas Propag.*, vol. 109, pp. 101–105, Aug. 2009.

[17] N. Forknall, R. Cole, and D. Webb, "Cumulative fading and rainfall distributions for a 2.1 km, 38 GHz, vertically polarized, line-of-sight link," *IEEE Trans. Antennas Propag.*, vol. 56, no. 4, pp. 1085–1093, Apr. 2008.

[18] C. Han, Y. Bi, and S. Duan, "Millimeter-wave propagation measurement during rainy days in Beijing," in *Proc. IEEE Int. Symp. Electromagn. Compat.*, May 2018, p. 73.

[19] H. J. Liebe, G. A. Hufford, and M. G. Cotton, "Propagation modeling of moist air and suspended water/ice particles at frequencies below 1000GHz," in *Proc. Effects Through Natural Man-Made Obscurants Visible MM-Wave Radiation*, May 1993, pp. 8–32.

[20] *(International Telecommunication Union Radio communication Bureau Propagation Recommendation), Attenuation by Atmospheric Gases*, document ITU-R P. 676-10, Sep. 2013.

[21] R. L. Olsen, D. V. Rogers, and D. B. Hodge, "The aR^b relation in the calculation of rain attenuation," *IEEE Trans. Antennas Propag.*, vol. 26, no. 2, pp. 319–329, Mar. 1978.

[22] *(International Telecommunication Union Radiocommunication Bureau Propagation Recommendation), Specific Attenuation Model for Rain for Use in Prediction Methods*, document ITU-R P. 838-3, Mar. 2005.

[23] R. Medhurst, "Rainfall attenuation of centimeter waves: Comparison of theory and measurement," *IEEE Trans. Antennas Propag.*, vol. 13, no. 4, pp. 550–564, Jul. 1965.

[24] *(International Telecommunication Union Radio communication Bureau Propagation Recommendation), Attenuation Due to Clouds and Fog*, document ITU-R P. 840-6, Sep. 2013.

[25] S. J. Niu, D. Y. Liu, L. J. Zhao, C. S. Lu, J. J. Lv, and J. Yang, "Summary of a 4-year fog field study in northern nanjing, part 2: Fog microphysics," *Pure Appl. Geophys.*, vol. 169, nos. 5–6, pp. 1137–1155, 1978.

[26] I. Gultepe, R. Tardif, S. C. Michaelides, J. Cermak, A. Bott, J. Bendix, M. D. Müller, M. Pagowski, B. Hansen, G. Ellrod, and W. Jacobs, "Fog research: A review of past achievements and future perspectives," *Pure Appl. Geophys.*, vol. 164, nos. 6–7, pp. 1121–1159, Jun. 2007.

[27] *(International Telecommunication Union Radiocommunication Bureau Propagation Recommendation), Propagation Data and Prediction Methods Required for the Design of Terrestrial Line-of-Sight Systems*, document ITU-R P. 530-13, Sep. 2013.

[28] T. Tjelta and D. Bacon, "Predicting combined rain and wet snow attenuation on terrestrial links," *IEEE Trans. Antennas Propag.*, vol. 58, no. 5, pp. 1677–1682, May 2010.

[29] K. Paulson and A. Al-Mreri, "A rain height model to predict fading due to wet snow on terrestrial links," *Radio Sci.*, vol. 46, no. 4, pp. 1–6 Aug. 2011.

[30] J. Ostrometzky, D. Cherkassky, and H. Messer, "Accumulated mixed precipitation estimation using measurements from multiple microwave links," *Adv. Meteorol.*, vol. 2015, Apr. 2015, Art. no. 707646. doi: 10.1155/2015/707646.

[31] S. Ishii, M. Kinugawa, S. Wakiyama, S. Sayama, and T. Kamei, "Rain attenuation in the microwave-to-terahertz waveband," *Wireless Eng. Technol.*, vol. 7, pp. 59–66, Apr. 2016.

[32] *Study on Channel Model for Frequencies from 0.5 to 100 GHz., Version 14.3.0*, document 3GPP TR 38.901, Dec. 2017.

[33] C. Moroder, U. Siart, C. Chwala, and H. Kunstmann, "Fundamental study of wet antenna attenuation," in *Proc. 15th Int. Conf. Environ. Sci. Technol.*, Sep. 2017, pp. 1–9.

[34] J. M. Garcia-Rubia, J. M. Riera, pp. Garcia–del-Pino, and A. Bernarroch, "Attenuation Measurements and Propagation Modeling in the W-Band," *IEEE Trans. Antennas Propag.*, vol. 61, no. 4, pp. 1860-1867, Apr. 2013.

[35] T. S. Rappaport, G. R. Maccartney, M. K. Samimi, and S. Sun, "Wideband millimeter-wave propagation measurements and channel models for future wireless communication system design," *IEEE Trans. Commun.*, vol. 63, no. 9, pp. 3029–3056, Sep. 2015.

[36] A. I. Sulyman, A. T. Nassar, M. K. Samimi, G. R. MacCartney, Jr., T. S. Rappaport, and A. Alsanie, "Radio propagation path loss models for 5G cellular networks in the 28 GHz and 38 GHz millimeter-wave bands," *IEEE Commun. Mag.*, vol. 52, no. 9, pp. 78–86, Sep. 2014.

[37] D. E. Berraki, S. M. D. Armour, and A. R. Nix, "Codebook based beamforming and multiuser scheduling scheme for mmWave outdoor cellular systems in the 28, 38 and 60GHz bands," in *Proc. IEEE Globecom*, Dec. 2014, pp. 382–387.

[38] J. Ostrometzky, A. Eshel, P. Alpert, and H. Messer, "Induced bias in attenuation measuremeommercial microwave links," in *Proc. IEEE Int. Conf. Acnd Signal Process. (ICASSP)*, New Orleans, LA, USA, May 2017, pp. 374–3744.

[39] S. Hur, T. Kim, D. J. Love, J. V. Krogmeier, T. A. Thomas, and A. Ghosh, "Millimeter wave beamforming for wireless backhaul and access in small cell networks," *IEEE Trans. Commun.*, vol. 61, no. 10, pp. 4391–4403, Oct. 2013.

[40] J. Ostrmetzky, R. Raich, L. Bao, J. Hansryd, and H. Messer, "The wet-antenna effect—A factor to be considered in future communication networks," *IEEE Trans. Antennas Propag.*, vol. 66, no. 1, Jan. 2018.

[41] *Study on New Radio Access Technology Physical Layer Aspects*, document 3GPP TR 38.802, Sep. 2017.

[42] S.-G. Park, V. N. Bringi, V. Chandrasekar, M. Maki, and K. Iwanami, "Correction of radar reflectivity and differential reflectivity for rain attenuation at X band. Part I: Theoretical and empirical basis," *J. Atmos. Ocean. Technol.*, vol. 22, pp. 1621–1632, Nov. 2005.

[43] S. Y. Matrosov, "Evaluating polarimetric X-band radar rainfall estimators during HMT," *J. Atmospheric Ocean. Technol., Amer. Meteorological Soc.*, vol. 27, pp. 122–137, 2010.

[44] S. Y. Matrosov, "X-band polarimetric radar measurements of rainfall," *Amer. Meteorological Soc.*, vol. 41, pp. 941–952, Sep. 2002.

[45] Y. Chen, J. Liu, S. Duan, D. Su, and D. Lv, "Application of X-band dual polarization radar in prediction estimation in summer of Beijing," *Climatic Environ. Res.*, vol. 17, no. 3, pp. 292–302, Apr. 2012.

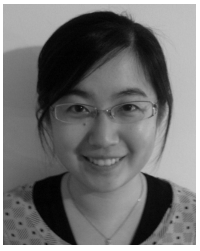

CONGZHENG HAN (M'04–SM'15) received the B.Eng. and Ph.D. degrees in electronic and communication engineering from the University of Bristol, U.K., in 2004 and 2009, respectively, where she was a Postdoctoral Research Staff with the Centre for Communication Research, from 2008 to 2011. Her Ph.D. degree was supported by the Dorothy Hodgkin Postgraduate Award and Toshiba Research Europe Ltd., U.K. She was a Spectrum Technology Specialist with the Office of Communications, U.K., from 2011 to 2014. She is currently a Research Fellow of the Institute of Atmospheric Physics, Chinese Academy of Sciences, China. She is also a Research Supervisor with the University of Chinese Academy of Sciences and the Chengdu University of Information Engineering, China. Her research interests include future generation wireless networks, green communications, environmental monitoring technology, and wireless energy harvesting.

SHU DUAN received the bachelor's degree in microwave engineering from the Department of Radio and Electronics, University of Science and Technology of China, Hefei, China, in 1982. He is currently a Professor Level Senior Engineer with the Key Laboratory of Middle Atmosphere and Global Environment Observation, Institute of Atmospheric Physics, Chinese Academy of Sciences, Beijing, China. He is also a Chief Scientist with the Jiangsu Key Laboratory of Meteorological Observation and Radar Technology. He invented the first *X*-band dual-polarized multi-static Doppler weather radar systems. His research interests include the areas of *X*-band dual-polarimetric radars, *X*-band dual-polarized Doppler weather radars, mesosphere–stratosphere–troposphere radars, and magnetron millimeter-wave cloud radars.